

Numerical modelling and finite element analysis of stress wave propagation for ultrasonic pulse velocity testing of concrete

Ismail Ozgur Yaman[†]

Middle East Technical University, Civil Engineering Department, Ankara, 06531, Turkey

Zekai Akbay[‡]

DaimlerChrysler AG, Truck Group, Sindelfingen, 71059, Germany

Haluk Aktan^{†‡}

*Wayne State University, Department of Civil and Environmental Engineering,
5050 Anthony Wayne Dr. #2164, Detroit, MI, 48202, USA*

(Received March 31, 2006, Accepted December 1, 2006)

Abstract. Stress wave propagation through concrete is simulated by finite element analysis. The concrete medium is modeled as a homogeneous material with smeared properties to investigate and establish the suitable finite element analysis method (explicit versus implicit) and analysis parameters (element size, and solution time increment) also suitable for rigorous investigation. In the next step, finite element analysis model of the medium is developed using a digital image processing technique, which distinguishes the mortar and aggregate phases of concrete. The mortar and aggregate phase topologies are, then, directly mapped to the finite element mesh to form a heterogeneous concrete model. The heterogeneous concrete model is then used to simulate wave propagation. The veracity of the model is demonstrated by evaluating the intrinsic parameters of nondestructive ultrasonic pulse velocity testing of concrete. Quantitative relationships between aggregate size and testing frequency for nondestructive testing are presented.

Keywords: concrete; nondestructive testing; ultrasonic pulse velocity; finite element analysis; explicit dynamic analysis; digital image processing; heterogeneous model.

1. Introduction

Stress wave propagation techniques are widely used in nondestructive evaluation of concrete members and structures. Among these, resonant frequency, ultrasonic pulse velocity (UPV), and impact-echo are the most common and standardized techniques (ASTM C 215, ASTM C 597, ASTM C 1383). UPV measurement is, however, one of the most commonly used stress wave

[†] Associate Professor, E-mail: ioyaman@metu.edu.tr

[‡] Manager, E-mail: zekai.akbay@daimlerchrysler.com

^{†‡} Professor, E-mail: haluk.aktan@wayne.edu

technique for nondestructive assessment of concrete properties both in the field and in the laboratory. The method is based on generating a stress wave (usually a P-wave) at ultrasonic frequencies at one boundary and measuring the time of arrival of the stress wave at another boundary. The UPV is then calculated from the time of arrival and an assumed wave path. The stress wave generation as well as the wave arrival time measurement is made using transducers with piezoelectric properties. The primary test parameters are the wave type, excitation frequency and amplitude. When compared to the UPV measurements on homogeneous materials like steel, the heterogeneous nature of concrete makes the transducer frequency selection more difficult and UPV measurement more challenging. For example, the excitation frequency needs to be much lower and the required pulsing energy needs to be much higher for concrete when compared to steel. Studies also document and demonstrate significant variability of the measured parameters such as UPV with changing concrete constituents, specifically the amount and type of coarse and fine aggregates, water-cement ratio (w/c), specimen age, volume of entrained air, and moisture state of concrete (Jones 1962, Yaman, *et al.* 2002a). Due to these variations, relatively simple testing procedures may require complicated data interpretation, interpretation by experienced personnel or sole reliance on empirical relations, all leading to a set of heuristically developed rules (rules developed by trial and error) for UPV testing. Consequently, analysis and testing applications cannot be generalized and remain limited to the specific specimen properties and purpose of the UPV testing.

Simulation of wave propagation in a heterogeneous medium, like concrete, is feasible and practical especially when appropriate finite element analysis platforms are used. The numerical simulations need to be an essential step in developing nondestructive test methods and selection of testing parameters; moreover, they can be useful for the enhancement of experimental applications. The efforts presented herein are directed towards developing and using numerical finite element analysis (FEA) of concrete, for the expressed purpose of establishing a framework for numerical simulation of stress wave propagation techniques that can be utilized for the quantitative evaluation of nondestructive testing methods.

2. Background

The first applications of the finite element method (FEM) for wave propagation simulation were in geophysics (Shipley, *et al.* 1967, Kuhlemeyer and Lysmer 1973). Shipley, *et al.* (1967) presented a comprehensive study of finite element simulation of elastic wave propagation for problems that have exact solutions. Based on the relationship between propagation velocity and wavelength, they indicated that finite element models of an elastic medium behave like low pass filters that have definite passing bands and cutoff frequencies. The band and cutoff frequencies are dictated by the finite element model, and its mesh size. In other words, stress waves beyond the cutoff frequency of the mesh cannot propagate through the finite element mesh. Kuhlemeyer and Lysmer (1973) stated that a reliable procedure for developing the finite element mesh for analysis of transient problems was not available. The standard technique used for assessing the adequacy of the finite element mesh is the patch-test where the element size is systematically reduced thus refining the mesh. They demonstrated the patch-test procedure on a study analyzing the accuracy of displacements generated by a single, harmonic, one-dimensional elastic wave propagating through a finite element mesh. By systematically reducing the element size of a homogeneous rod model from one-fourth to one-twelfth of the wavelength of the propagating wave, the error in the displacement field monotonically

decreased from 4% to 1%. To further decrease the error in the displacement field, the use of consistent mass matrix formulation was suggested.

National Institute of Standards and Technology and Cornell University researchers performed FEA simulation of wave propagation in concrete structures. Sansalone, *et al.* (1987) used finite element (FE) models to simulate the response of concrete structures to elastic impact. Starting with a simple problem of wave propagation in a concrete plate, they simulated planar flaws assuming concrete as a linear, homogeneous, and isotropic material. The concrete plate was modeled using 2D-plane strain elements. They described the FEM as a valuable tool for understanding the interaction of stress waves within solids with defects. Lin and Sansalone (1992) also used 2D and 3D FE models to investigate the transient elastic response of thick circular, square and rectangular bars subjected to transverse point impact. The findings from these studies were synthesized to establish a basis for using the impact-echo technique for nondestructive evaluation of bar-like elements such as columns and beams. Sansalone (1997) summarized the work carried out to successfully implement the impact-echo method on concrete structures and pointed out the importance of using FE based computer models for simulating the response of structures subjected to elastic impact.

In all of the above mentioned applications, concrete was modeled as a homogeneous isotropic material. In this study, an advancement of FE modeling is described in which the concrete is modeled as a composite material consisting of different phases. The composite structure of concrete is described by Wittmann (1985) in a "Three-level-approach". Wittmann assumed that the material structure of concrete can be divided into three hierarchical levels, micro-, meso- and macro-, with each level described by characteristic features and mechanisms. For example, in micro level models the structure of the cement paste is described for modeling mechanisms such as capillary tension and disjoining pressure. Whereas, the meso-structural level, which is appropriate for wave propagation modeling, the effect of pores, inclusions, and cracks are the primary characteristic features of concrete as a composite material.

Following Wittmann's hierarchical approach, wave propagation analysis in concrete can be simulated by different modeling levels. In the macro-level, concrete can be modeled as a homogeneous material with isotropic properties and the overall structural response to boundary impact can be simulated. In modeling, verifying, and calibrating nondestructive evaluation techniques on concrete, the meso-level material response can be crucial. In that case, concrete can be modeled as a heterogeneous material composed of mortar and aggregate phases each with unique properties. With the meso-level FE models, the effects of aggregate content, shape and modulus can be analyzed. Models can also be developed at the micro-level, to investigate the effects of changing moisture by absorption and desorption within the microstructure of hydrated cement as influenced by w/c (Yaman 2002a and b).

3. Simulation by finite element analysis (FEA)

Measurement of the UPV of concrete specimens is the most widely used stress wave propagation technique. UPV is the velocity of a group of stress waves, primarily the compression or P-waves, through concrete that propagate at frequencies within the ultrasonic range. The UPV testing is usually performed using two transducers; with one applying a pulse at a boundary and the other recording the wave arrival at another boundary of the specimen. The common equipment used for UPV measurement includes piezoelectric transducers, a pulser/receiver and an oscilloscope

commonly integrated with a computing package. In this article, ultrasonic P-wave propagation within a 100 mm diameter and 200 mm long concrete specimen will be simulated to represent the UPV measurement process. The simulations will be utilized to investigate the intrinsic parameters of FEA and later the intrinsic parameters of concrete for UPV testing.

UPV measurement on a concrete specimen can be simulated numerically by the direct integration of dynamic response equation. Using the direct integration method of analysis, the vibration response time history at one spatial coordinate of the structure is obtained using a numerical step-by-step integration procedure. This step-by-step numerical procedure may be performed using either an implicit or explicit integration scheme (Chopra 1995).

In the implicit integration scheme, the displacement response is calculated when the dynamic response equation satisfied at time “ $t+\Delta t$ ”. This necessitates the inversion of the effective stiffness matrix which is a computationally intensive step. The stiffness matrix can be made positive definite, thus invertible, by modeling the specimen with boundary conditions to form a stable structure. Nevertheless, the implicit integration scheme is computationally intensive, especially for large degree of freedom (DOF) systems. However, due to the fact that equilibrium is satisfied at the time step that the response is sought ($t+\Delta t$); this integration scheme is “unconditionally stable”. Implicit schemes are not preferred in wave propagation analysis not only due to the computational intensity, but also due to test specimens being modeled as unstable structures. For example, during the resonant frequency testing of a concrete specimen, the specimen is suspended at midpoint, thus forming an unstable structure (ASTM C215). The stiffness matrix of FE models of unstable structures will not be positive definite which is essential for implicit wave propagation analysis. Because of the abovementioned facts, wave propagation analysis cannot be practically performed with implicit integration schemes.

In explicit integration scheme, dynamic response equation is satisfied at time “ t ” to evaluate the response at time “ $t+\Delta t$ ”. This scheme is formulated by the inversion of the effective mass matrix, which is symmetric, making the use of explicit integration attractive for large DOF systems. However, the scheme is not “unconditionally stable” and a maximum integration time increment limitation is imposed to assure stability of the numerical solution. If the time increment (step) is greater than a critical value, Δt_{cr} , there is no assurance that the numerical integration will remain stable. Hence, the explicit integration scheme is categorized as “conditionally stable” with a limiting time step called the stability limit.

The stability limit Δt_{cr} is defined in terms of the highest frequency of the FE model of the structure and given as (Bathe 1996):

$$\Delta t_{cr} = \frac{2}{\omega_{\max}} = \frac{T_{\min}}{\pi} \quad (1)$$

where, ω_{\max} is the highest frequency and T_{\min} is the corresponding minimum period of the FE system. The value of T_{\min} or ω_{\max} is determined by modal analysis of the full FE model. Alternatively, a simple estimate of the highest frequency of each element (ω_{\max}^{el}) in the model can be an efficient and a conservative approximation of ω_{\max} . Since, $(\omega_{\max}^{el})_{\max}$ is always greater than ω_{\max} (Bathe 1996). Therefore, an estimate of the stability limit can be defined based on the smallest element length (L^e) utilized in the FE mesh, and the compression wave or P-wave velocity of the material (V_p) as:

$$\Delta t_{cr} = \frac{(L^e)_{\min}}{V_p} \quad (2)$$

For example, in meshing a cylindrical specimen, if the smallest element dimension is 3 millimeters and the P-wave velocity is estimated as 4000 meters/second, the largest integration time step that assures a stable solution will be 0.75 microseconds. This definition of the stability limit enables the selection of an appropriate time step for accurate response calculation. If a time step larger than Δt_{cr} is used in the analysis, the integration may become unstable, resulting in a divergent solution.

3.1. Homogeneous (Smearred) finite element models

The parameters involved in the wave propagation analysis of a FE model are investigated first by homogeneous finite element models. The FEA parameters are the integration time step, mesh size, and integration scheme. Whereas, in wave propagation analysis the parameters are frequency, wavelength, and wave velocity. As discussed earlier, these parameters are not independent, for example, the integration time step is a function of both the mesh size and the integration scheme. The wave propagation parameters of velocity, wavelength, and frequency are also related.

These parameters are investigated using the computer simulations of: an ultrasonic through-transmission testing of a cylindrical specimen of length 200 mm and radius of 400 mm. A specimen with larger radius than length is defined in order to minimize the effect of specimen shape on wave velocity. Concrete is modeled as a homogeneous, linear, elastic, and isotropic material. Utilizing radial symmetry, the three-dimensional specimen will be reduced to a two-dimensional model using axisymmetric elements. The density (ρ), modulus of elasticity (E), and Poisson's ratio (μ) selected are 2200 kg/m³, 49.5 GPa, and 0.2, respectively. The theoretical P-wave velocity (V_p) is calculated as 5000 m/s from the equation below:

$$V_p = \sqrt{\frac{E(1-\mu)}{\rho(1+\mu)(1-2\mu)}} \quad (3)$$

The excitation applied on the specimen is sinusoidal with a frequency of 50 kHz and duration of 80 μ sec to simulate the input from the pulser transducer. The pulse is applied as prescribed displacements 0.001 micrometers on specific boundary nodes. The actual magnitude of the displacement field imposed by the pulsing transducer during ultrasonic testing is known to be very small, but specific values are not measured and reported. Symmetry boundary conditions are used for the axisymmetric model of the concrete specimen (Fig. 1a). The pulser transducer with a 50 kHz central frequency is modelled to apply a steady state dynamic loading at the associated node as shown in Fig. 1(b). The receiving transducer output is defined as the response of the specimen as measured at the bottom boundary of the specimen. A typical response plot is provided in Fig. 1(c).

The FEA is performed using Version 6.1 of ABAQUS specific to explicit integration (ABAQUS/Explicit 2000). The cylindrical specimen is meshed using axisymmetric, reduced integration, continuum elements (CAX4R). ABAQUS/Explicit element library includes reduced integration elements for efficient utilization of the explicit integration scheme. Reduced integration elements use a lower-order integration (1 point only) to form the element stiffness, thus reducing the computational time. The drawback of the reduced integration elements is the numerical instability of the analysis illustrated as "hourglassing". Hourglassing is the numerical instability caused by the non-straining deformations of finite elements. In other words, with reduced integration points the elements may distort in such a form that the strains at the integration points will remain zero. The potential for hourglassing increases as the number of integration points within the finite element is

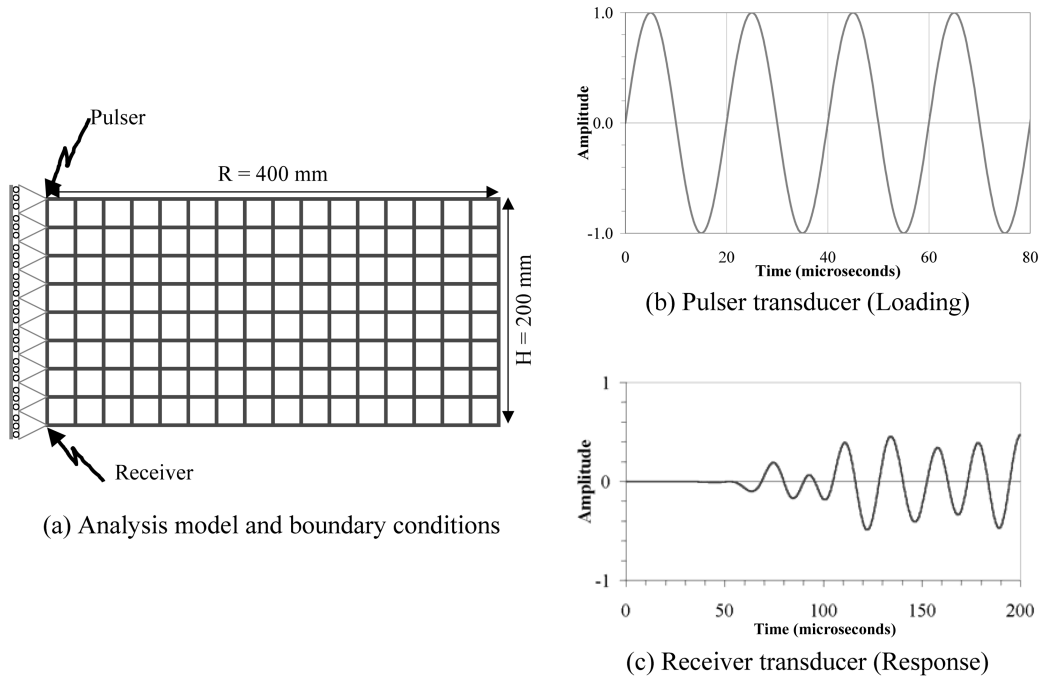


Fig. 1 Schematic representation of the FEA procedure

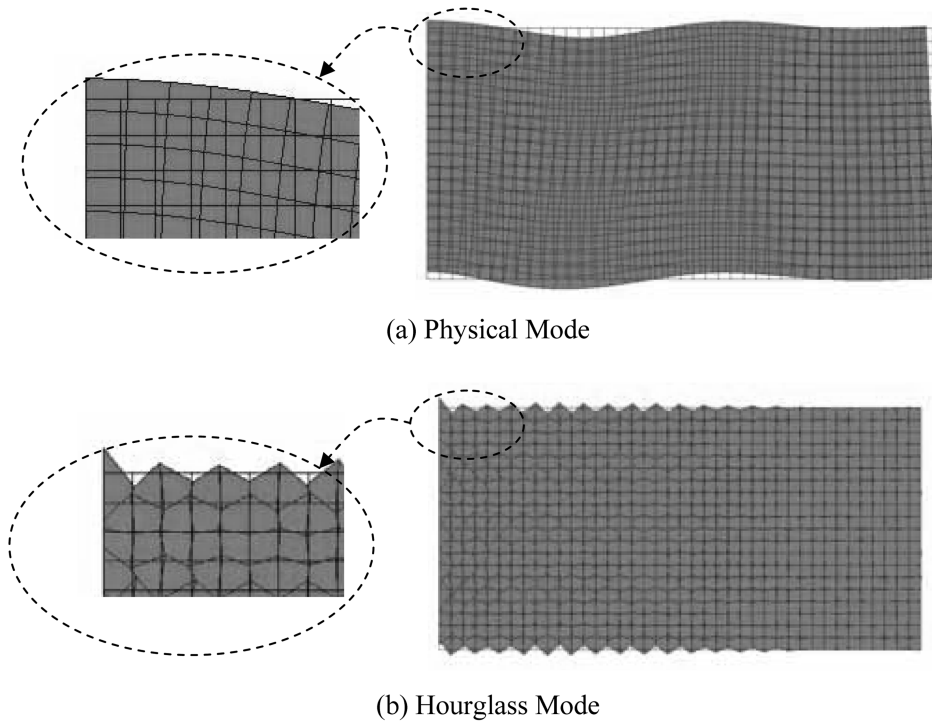


Fig. 2 Depiction of the hourglass mode against a physical mode of the specimen

reduced. As an example, Fig. 2 presents two modal shapes of the concrete specimen axisymmetric model. The first mode is a normal (physical) while the second mode is an hourglass (non-physical or zero-energy mode). ABAQUS/Explicit also includes a defense by introducing an artificial “hourglass stiffness” in the element formulations, which limits the propagation of this non-physical deformation (ABAQUS/Explicit2000).

The FE models developed are six decreasing sizes of square mesh corresponding to element sizes (L^e) of 100, 50, 20, 10, 5, and 2.5 mm. These mesh sizes result in a total of 8, 32, 200, 800, 3200, and 12800 elements correspondingly, to define the FE model. The stability time limit (Δt_{cr}) corresponding to each finite element is selected as the time of a P-wave to traverse that particular element as defined in Eq. (2). Analysis is performed for each mesh size using five different

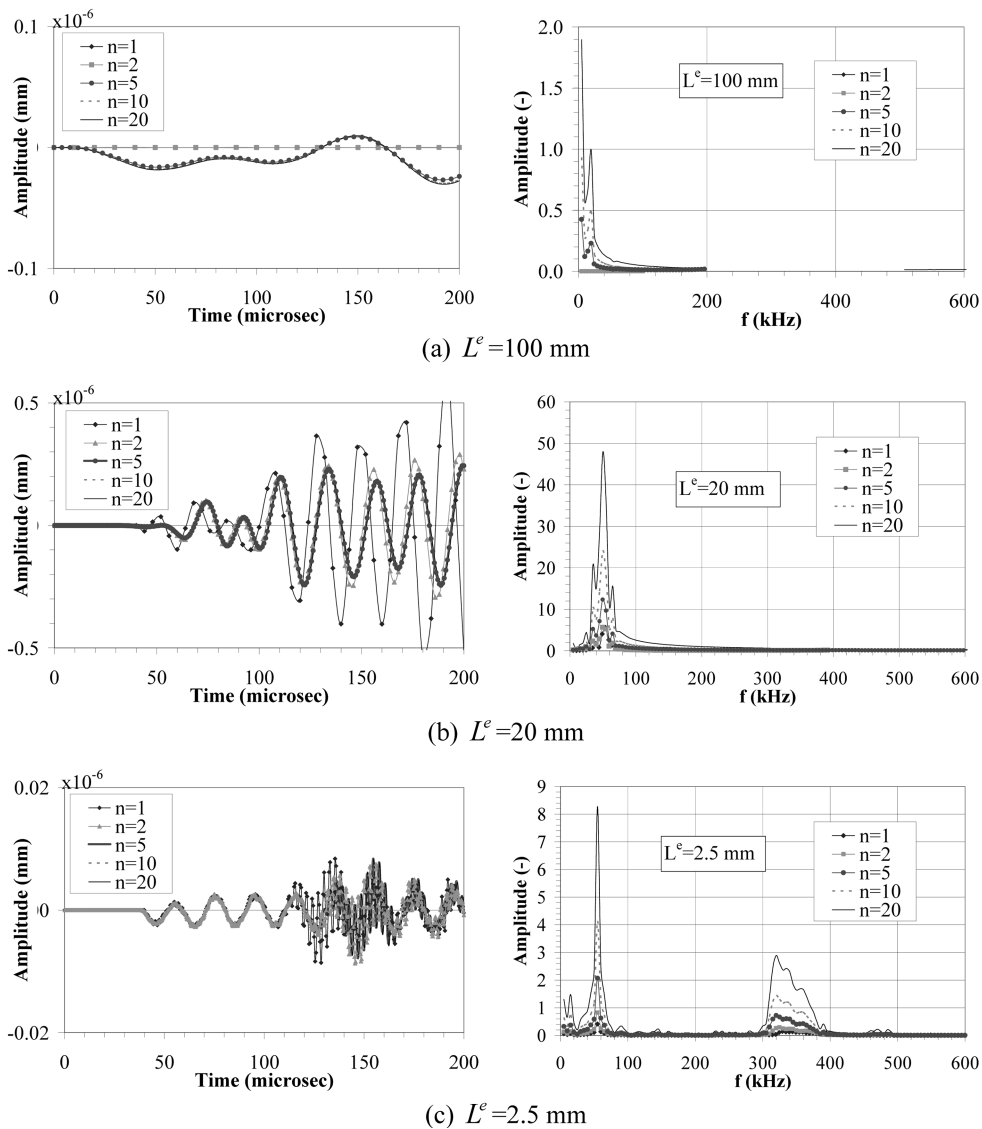


Fig. 3 Effect of time step and element size on the FEA

integration time steps (Δt). Each time step is selected as an increasing ratio (n) of the stability time limit as: $\Delta t_{cr}/\Delta t = 1, 2, 5, 10,$ and 20 , generating thirty solutions.

The effect of integration time-step on the calculated wave amplitude accuracy is examined in Figs. 3(a) through 3(c). The figures show the a family wave time histories, corresponding to five different integration time steps, received at the location of the receiving transducer for the FE meshes with (L^e) of 100, 20, and 2.5 mm. Also shown in these figures are the frequency domain counterparts of the waveforms. Note that in these figures the y-axis scale is not kept uniform in order to have the waveform amplitudes appear uniform. As seen from the waveforms in the time domain, as n increases from 1 to 20, the solution accuracy improves independent of the mesh size. Moreover, as the mesh size is reduced, the solution becomes unstable when integration time step is equal to the stability limit ($n=1$). The amplitude response shown in Fig. 3(c) diverges beyond a certain time (around 120 μ sec). The implications of the divergence of the FE solution will be discussed later in the article.

As mentioned earlier, the calculated waveform amplitudes vary significantly as L^e is changed. Comparing the wave amplitudes in Figs. 3(a) through 3(c) the largest are with the element size of 20 mm. For large element sizes (Figs. 3a), small wave amplitudes are expected as the FE model does not possess the modes of interest, i.e., the applied wave frequency of 50 kHz. This agrees with the observations of Shipley, *et al.* (1967) that FE models behave like low pass filters. Since the cutoff frequency of the model was less than 50 kHz, responses beyond that frequency cannot be generated. As the cutoff frequency of the FE model is increased, by decreasing L^e , the model will be capable of calculating wave amplitudes within the range of the true solution. This is the case for waveforms in Fig. 3(b) and (c), but not for Fig. 3(a).

For the interpretation of the increasing waveform amplitudes in Fig. 3(b) the analysis results are displayed in the frequency-domain as shown in the second column of Figs. 3(a)-(c). The amplitudes associated with frequencies of all the FE analysis except the coarse mesh (L^e of 100, Fig. 3a) includes a peak around 50 kHz, which is the excitation frequency. This excitation frequency cannot be simulated with the FE models with a coarse mesh, as they possess only the frequency (cutoff frequency) response modes lower than 50 kHz. On the other hand, the amplitudes of FE models with the finer mesh, shows a second peak beyond the testing frequency. This frequency associated with the second peak changes with L^e and shifts to a higher frequencies (around 85 kHz for 10 mm, 170 kHz for 5 mm, and 330 kHz for 2.5 mm element sizes) with reducing L^e . The second peak is arising from the wave reflection from the element boundaries and is termed as “ringing frequency” thus controlled by the FE discretization. A consequence of the wave reflection from the element boundaries is that, part of the wave energy gets trapped causing the reduction in amplitudes as the wave propagates through FE boundaries. In FE models with finer meshes, with increasing number of element boundaries, the wave amplitudes gradually decrease as seen in Fig. 3. The maximum wave amplitudes are observed in the mesh sizes where the testing frequency and the ringing frequency match, in this case the 20 mm mesh. Consequently, in specifying the maximum mesh size of the FE model, excitation frequency should also be considered. Additionally, the resulting wave motion needs to be filtered from the artificial frequency generated by reflection from the element boundaries. It should be noted that energy-absorbing boundary elements can be used to eliminate this artificial frequency. This option was not explored in this study in order to retain the similitude between the real specimen and its FEA model.

The wave motion calculated by the FEA is also used to verify the relationship between wave velocity, frequency, and wavelength. For this purpose the ultrasonic wave velocity is computed from

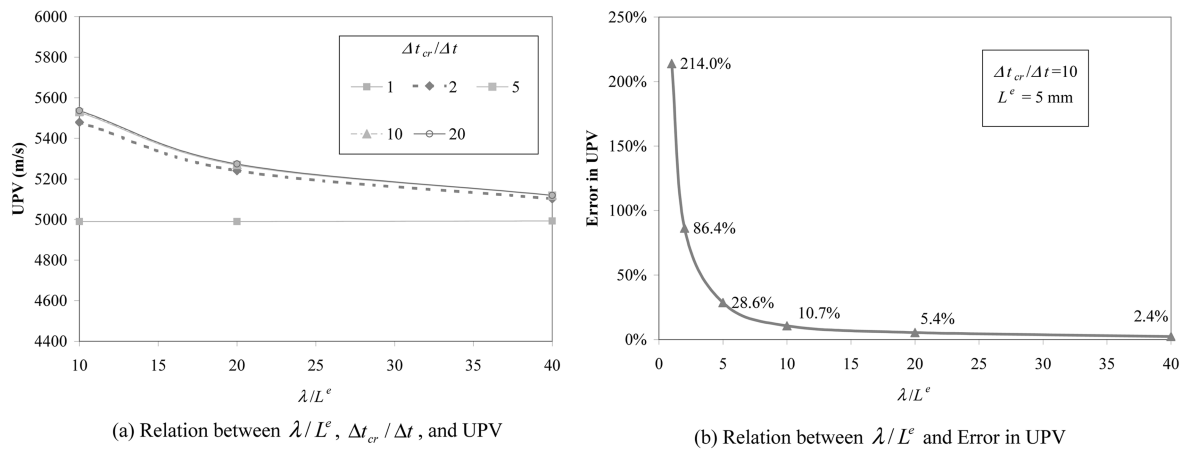


Fig. 4 Analysis parameters for the FE model with $L^e=5$ mm

the calculated wave motion shown in Figs. 3(a)-(c) arriving at the specimen base boundary. The wave time-of-flight is computed from the FEA results using the time-of-flight measurement procedure developed by Yaman, *et al.* (2001). The UPV is calculated and plotted against λ/L^e and $\Delta t_{cr}/\Delta t$ in Fig. 4(a), where λ is the wavelength. As seen from the figure, with increasing λ/L^e ratio, the calculated UPV approaches its theoretical UPV of 5000 m/s. For a $\Delta t_{cr}/\Delta t$ ratio of 10, the difference in the calculated UPV is plotted in Fig. 4(b). As an example, the analysis using a λ/L^e ratio of 20 results in a difference of 5.4% in UPV. This difference is primarily due to the error in the wave time-of-flight calculation and in part due to the numerical noise generated in the FE analysis. The wave arrival time measurement incorporates another error source, which is the numerical noise generated by the round-off error.

The FE model with the element size of 5 mm is reanalyzed using the implicit code of ABAQUS/Standard. The purpose of this analysis is to verify the accuracy of the explicit integration scheme and the reduced integration elements. In this analysis integration time increment is selected as $\Delta t_{cr}/10$ and axisymmetric continuum (CAX4) elements are used. Unlike CAX4R, CAX4 continuum elements utilize full integration points, eliminating the possibility of hourglassing deformations. ABAQUS/Explicit results gave a very close match to the waveform obtained using ABAQUS/Standard with full-integration elements (CAX4). The analysis using the ABAQUS/Implicit on a dedicated workstation took ten hours to complete versus twenty minutes with the explicit version, a significant difference in computational effort.

The concern in using the explicit integration scheme is the numerical instability of the solution. The numerical stability of the solution can be identified by monitoring the energy balance during the FEA of the wave propagation. Theoretically, in a linear elastic system, input energy must balance the stored energy, giving a zero energy balance. Numerical instability of the response will generate unaccounted differences in the energy balance. These unexpected differences in the energy balance are warning signs for a time increment that is too large for assuring a stable solution (ABAQUS 2000). Therefore, energy balance of an explicit solution is usually monitored. As an example, the FEA with an element size of 5 mm for two different time increments (Δt_{cr} and $\Delta t_{cr}/10$) are performed. The analysis using an integration time equal to Δt_{cr} start to deviate from the analysis using an integration time step of $\Delta t_{cr}/10$ after about 100 microseconds as shown in Fig. 5(a). The divergence of the explicit solution is explained by the energy balance plot (Fig. 5b) showing a nonzero energy balance.

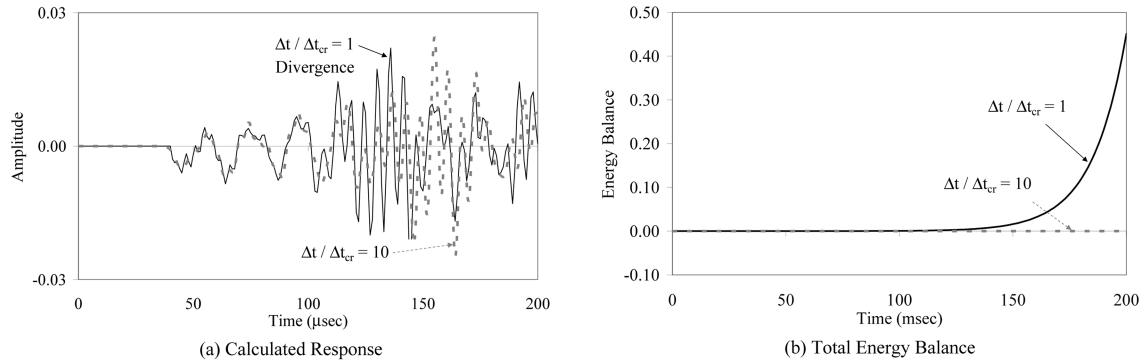


Fig. 5 Energy balance against time to assess the stability of the FEA solution with $L^e=5$ mm

3.2. Heterogeneous (Two-phase) finite element models

Examining a concrete cross-section, the heterogeneity of the concrete material structure becomes obvious. At the macro level, the aggregates of different shapes and sizes are embedded in a mortar matrix. The complexity increases when the concrete material is examined at the micro level. Pores of different shapes, sizes, and tortuosity as well as the interface between the aggregate and the cement paste contribute to the structural complexities of the concrete material. In modeling the concrete medium for wave propagation analysis, an alternative structural model, is to represent the macrostructure of concrete as consisting of mortar and an aggregate phase. The meso-level properties such as the capillary pores and entrained air pores can be incorporated in describing the mortar properties. Material models for computing the mortar properties at different porosities are discussed in the literature (Yaman, *et al.* 2002a, 2002b). Using these models, the entrained air and capillary pores including the moisture state can be incorporated with the mortar properties.

FE modeling of heterogeneous (two-phase) concrete models is performed to analyze the influence of excitation frequency on ultrasonic pulse velocity (UPV) of a concrete specimen. In literature, there is conflicting information on the relationship between test frequency and constituent size. For example, in ultrasonic testing of concrete, the relationship between frequency and the constituent size is not discussed in ASTM C 597. However, for rock specimens, ASTM D 2845 recommends that the wavelength of the ultrasonic waves used in testing should be at least three times greater than the average grain size. In order to evaluate the effect of excitation frequency, FEA is performed for investigating the wave scattering phenomena in a heterogeneous concrete model.

The FE mesh is developed by defining the geometry of the aggregate inclusions within a mortar matrix of a concrete section by image processing of the digital photographic image. First, for each digital image of a concrete section, aggregate and mortar phases are identified by the enhancement of the coarse aggregate images. Second, a filtering process is utilized to construct a clear contrast between the mortar and the aggregate border. There are numerous image processing software available for such applications. The processing performed in this study is very basic thus any commercial software such as the Matlab Image Processing Toolbox would be able to provide the means to differentiate between the mortar and aggregate phases. In the final step, the processed digital image is mapped on a FE mesh with aggregate and mortar as two different material types. The original digital images of two actual $\phi 100$ mm by 200 mm concrete test specimens and the associated FE models for two specimens are presented in Fig. 6.

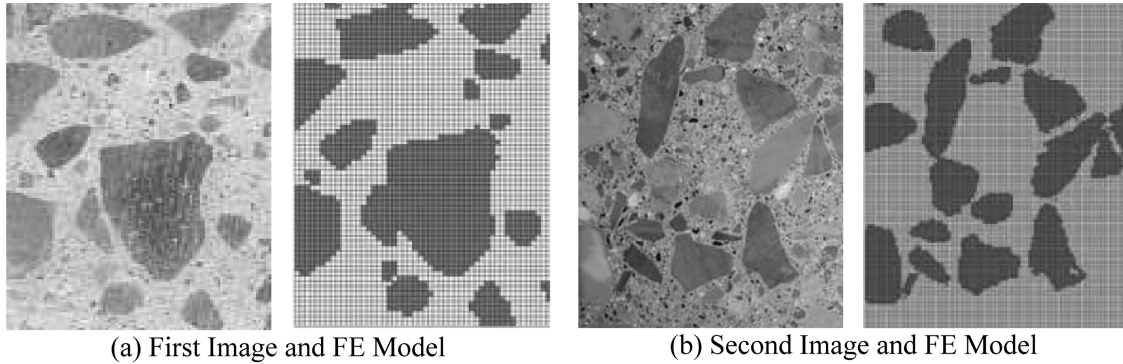


Fig. 6 Digital images of two actual specimens and corresponding FE models

Table 1 Mortar and aggregate properties for the heterogeneous models

Property	Mortar	Aggregate
Density (kg/m^3)	2350	2600
Elasticity Modulus (GPa)	26.9	85.0
Poisson's Ratio	0.22	0.15

Table 2 FEA parameters for both of the heterogeneous models

Model	λ (mm)		Δt_{cr} (μsec)		# of Elements		L^e (mm)	Δt (μsec)
	Mor.	Agg.	Mor.	Agg.	Mor.	Agg.		
1	72	118	0.27	0.17	6644	4068	0.97	0.01
2	72	118	0.28	0.17	6202	3798	1.00	0.01

The two FE models are generated from the digital images taken from two actual specimens being tested as part of an experimental program (Yaman, *et al.* 2002a, 2002b). The mechanical properties of the constituents are shown in Table 1, and the FE model properties are given in Table 2, showing the element size, approximate wavelengths for mortar and aggregate elements, and the critical time step (Δt_{cr}). Using the findings of the analysis of homogeneous models, an integration time step of $\Delta t=0.01$ microseconds and mesh size of $L^e=1.0$ mm were used in the FE analysis of the heterogeneous models. This element length corresponds to a λ/L^e of 72 and an integration time step of $n=17$.

The relationship between the excitation frequency and constituent size is investigated using the two-phase FE model subjected to ultrasonic pulses of frequencies 50, 100, 150, 250, and 500 kHz. Standard cylindrical specimens with a diameter of 100 mm and a length of 200 mm are modeled using CAX4R elements similar to the analysis performed with the homogeneous models. Similar to homogenous models, a pulser transducer is simulated with a 50 kHz loading uniformly applied within the radius of the transducer, i.e., 25 mm. The wave response at the other surface of the specimen is averaged as the receiving transducer output.

The waveforms representing the wave motion arriving at the specimen base, for all of the five excitation frequencies are shown in Figs. 7(a)-(e). These figures include time and frequency domain representations corresponding to excitation frequencies of 50 to 500 kHz. For purposes of joint

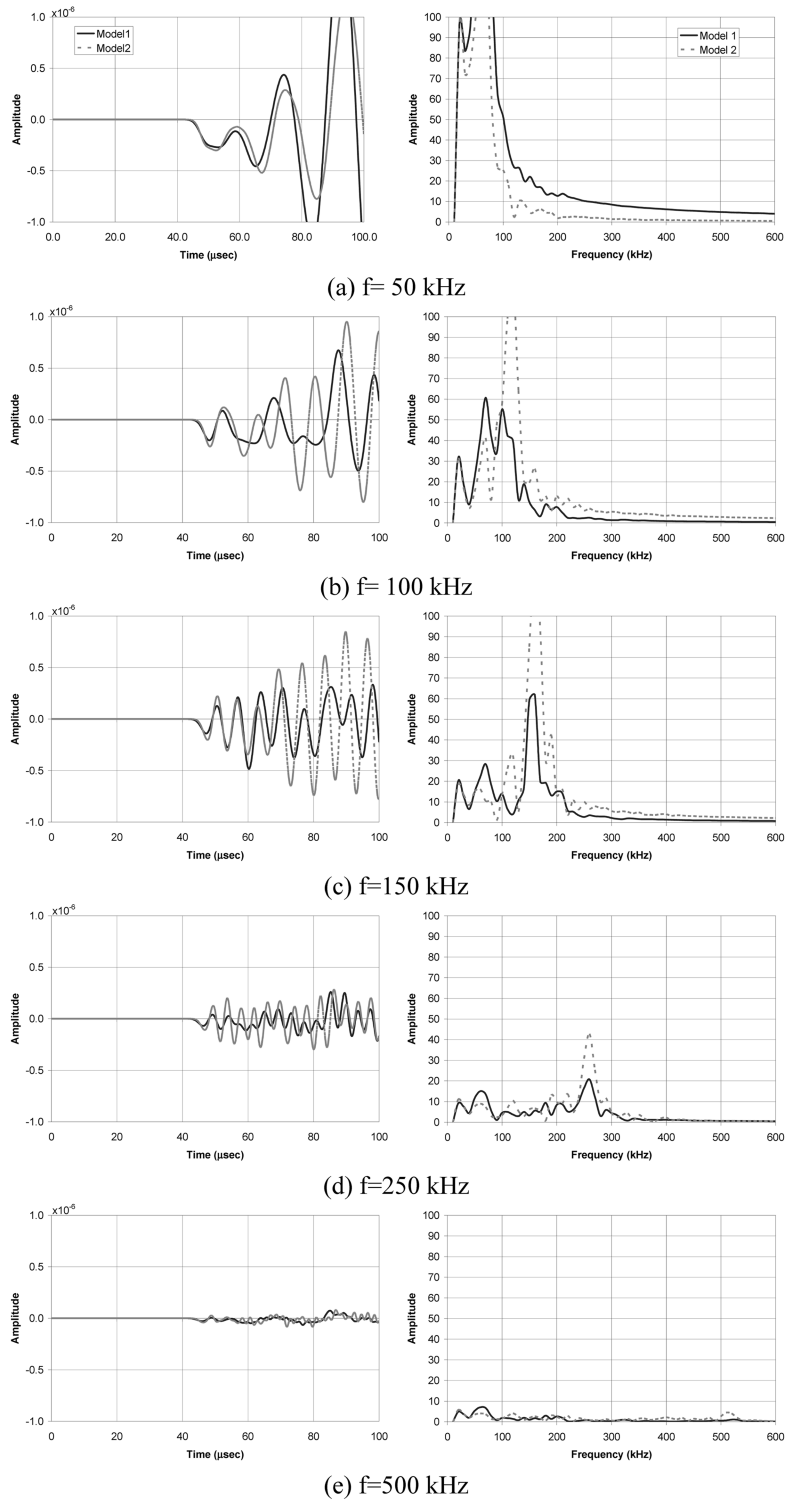


Fig. 7 Effect of testing frequency and constituent size

comparison of all the testing frequencies, the amplitude scales are normalized. A decrease in waveform amplitudes with increasing excitation frequency is observed as the reduction in wave energy due to the scattering from aggregate boundaries. Also seen in the frequency domain representations of wave time histories in Fig. 7(a)-(c), the excitation frequencies between 50 kHz through 150 kHz provide reasonable wave amplitudes at the location of the receiving transducer. Under excitation frequencies of 250 kHz and 500 kHz, the wave motion attenuates and the wave amplitudes at the receiving transducer location are very low. The average aggregate size represented in the FE model is about 20 mm and the UPV calculated from the time of flight is 4500 m/s. The excitation frequencies of 50 kHz and 100 kHz generate waves with wavelengths around 90 mm and 45 mm, respectively. Keeping in mind that the experimental errors generated in an actual experiment is absent in numerical simulation, testing frequencies of 50 kHz and 100 kHz would be appropriate for UPV measurement of concrete. In fact, 50 kHz and 100 kHz are the test frequencies often used for UPV testing of concrete (Jones 1962). At these frequencies wavelength will be close to three times the average aggregate size, as recommended by ASTM D2845.

4. Summary and conclusions

The development of finite element modeling, simulation and analysis procedure in UPV testing of concrete is presented. The UPV measurement is used as the highlighted stress wave propagation technique in discussing finite element analysis parameters and their relationship with testing parameters. Also discussed is the development of homogeneous (smeared) and heterogeneous (two-phase) material models of concrete for simulating wave propagation during ultrasonic testing. ABAQUS/Explicit version of the finite element analysis package is utilized and explicit integration scheme is recommended as an appropriate solution procedure for wave propagation in concrete medium. Finite element analysis parameters (element size and integration time increment) in simulation of wave propagation in concrete medium are investigated, and recommendations are made for their selection. The relationship between finite element size and integration time increment, and element size and testing frequency is clarified. Development of a two-phase heterogeneous concrete material model is presented. A digital image processing methodology is identified and utilized for differentiating between the mortar and aggregate phases of digital photographic images of concrete sections. With this methodology the mortar and aggregate phases are identified from digital images, and mapped directly to generate the finite element model mesh. This FE model is then used in demonstrating the influence of aggregate sizes on the ultrasonic testing of concrete, in terms of testing frequency.

The contents of this paper help us to conclude following points:

1. The explicit finite element analysis method is an efficient solution technique for simulating wave propagation in a concrete medium if, analysis parameters like element size and integration time increment is defined rationally.

2. The element size in finite element mesh, the integration time increment selected for numerical simulation of the testing, and the frequency characteristic of the actual testing are all inter-related parameters. The maximum permissible element size in the FE mesh is dependent on the excitation frequency and the wavelength of the stress wave. For a selected λ/L^e ratio of 40 (when the wavelength is divided into 40 elements), the wave velocity is computed with an error of 2.4% from the actual wave velocity.

3. It is important to keep in mind that the selection of the integration time increment is dependent on the element size, and a $\Delta t_{cr}/\Delta t$ ratio of at least 5 should be used for the element type described in this study.

4. Digital image processing techniques can be used for accurately identifying the non-homogenous components of the concrete material and for transferring the images to finite element models. The heterogeneous (two-phase) models developed in this paper in conjunction with utilization of the finite element analysis allowed establishing a rational relation between the testing frequency and the aggregate size.

5. Heuristically developed rules of ultrasonic testing for concrete can be assessed effectively using the two-phase finite element analysis models. Numerical simulations performed in this study showed that testing frequencies between 50-150 kHz allow ultrasonic wave to propagate through the concrete medium of 20 centimeter in length in the direction of the wave, whereas frequencies greater than 150 kHz could not fully propagate.

Notation

The following symbols are used in this paper:

ρ	: Density
E	: Modulus of elasticity
μ	: Poisson's ratio
V_p	: P-wave velocity
t	: Integration time
Δt	: Integration time increment
Δt_{cr}	: Critical integration time increment (stability limit)
ω_{max}	: Highest frequency of the finite element model
T_{min}	: Lowest period of the finite element model
ω_{max}^e	: Highest frequency of the finite element
L^e	: Finite element length
λ	: Wavelength

References

- ABAQUS User's Manual Ver. 6.1*, Hibbitt, Karlsson, & Sorensen Inc., 2000.
- ASTM C215 (2004), "Standard test method for fundamental transverse, longitudinal, and torsional frequencies of concrete specimens", *American Society for Testing and Materials*, West Conshohocken, Pennsylvania, Vol. 04.02, .
- ASTM C 597 (2004), "Standard test method for pulse velocity through concrete", *American Society for Testing and Materials*, West Conshohocken, Pennsylvania, Vol. 04.02.
- ASTM C1383 (2004), "Standard test method for measuring the p-wave speed and the thickness of concrete plates using the impact-echo method", *American Society for Testing and Materials*, West Conshohocken, Pennsylvania, Vol. 04.02.
- ASTM D2845 (2004), "Standard test method for laboratory determination of pulse velocities and ultrasonic elastic constants of rock", *American Society for Testing and Materials*, West Conshohocken, Pennsylvania, Vol. 14.02.

- Bathe, K.J. (1996), *Finite Element Procedures*, Prentice Hall Inc., New Jersey.
- Chopra, A.K. (1995), *Dynamics of Structures*, Prentice-Hall Inc., New Jersey.
- Jones, R. (1962), *Non-destructive Testing of Concrete*, Cambridge University Press.
- Kuhlemeyer, R.L. and Lysmer, J. (1973), "Finite element accuracy for wave propagation problems (Technical Note)", *J. Soil Mech. Found. Div., Proc. ASCE*, **99**(SM5), pp. 421-427.
- Lin, Y. and Sansalone, M. (1992), "Transient response of thick circular and square bars subjected to transverse elastic impact", *Journal of Acoustical Society of America*, **91**(2), pp. 885-892, February.
- Mehta, P.K. and Monteiro, P.J.M. (1993), *Concrete: Structure, Properties, and Materials*, Second Edition, Prentice-Hall Inc., New Jersey.
- Sansalone, M. (1997), "Impact-echo: the complete story", *ACI Struct. J.*, **94**(6), pp. 777-786, November-December.
- Sansalone, M., Carino, N.J. and Hsu, N.N. (1987), "A finite element study of transient wave propagation in plates", *Journal of the National Bureau of Standards*, **92**(4), pp.267-278, July-August.
- Shibley, S.A., Leistner, H.G. and Jones, R.E. (1967), "Elastic wave propagation-a comparison between finite element predictions and exact solutions", *Proc. International Symposium on Wave Propagation and Dynamic Properties of Earth Materials*, University of New Mexico Press, Albuquerque, pp. 509-519.
- Tedesco, J.W, McDougal W.G and Ross, C.A. (1998), *Structural Dynamics: Theory and Applications*, Addison Wesley Longman Inc.
- Wittmann, F.H. (1985), "Deformation of concrete at variable moisture content", *Mech. Mater. Ed. Z. Bazant*, John Wiley and Sons Ltd.
- Yaman, I.O., Aktan, H. and Hearn, N. (2002a), "Active and non-active porosity in concrete Part I: Experimental evidence", *Mater. Struct.*, **35**(246), pp. 102-109, March.
- Yaman, I.O., Aktan, H. and Hearn, N. (2002b), "Active and non-active porosity in concrete Part II: Evaluation of existing models", *Mater. Struct.*, **35**(246), pp. 110-116, March.